



## Flavin mimetics: Synthesis and photophysical properties

Dora-M. Rășădean<sup>a</sup>, Takashi Machida<sup>b</sup>, Kazuki Sada<sup>c,d</sup>, Christopher R. Pudney<sup>e</sup>,  
G. Dan Pantoș<sup>a,\*</sup>

<sup>a</sup> Department of Chemistry, University of Bath, Claverton Down, Bath, BA2 7AY, UK

<sup>b</sup> International Center for Materials Nanoarchitectonics (WPI-MANA), National Institute for Materials Science (NIMS), 1-1 Namiki, Tsukuba, 305-0044, Japan

<sup>c</sup> Graduate School of Chemical Sciences and Engineering, Hokkaido University, Kita 10 Nishi 8, Kita-ku, Sapporo, Japan

<sup>d</sup> Department of Chemistry, Faculty of Science, Hokkaido University, Kita 10 Nishi 8, Kita-ku, Sapporo, Japan

<sup>e</sup> Department of Biology and Biochemistry, University of Bath, Claverton Down, Bath, BA2 7AY, UK

### ARTICLE INFO

#### Article history:

Received 30 November 2020

Received in revised form

29 December 2020

Accepted 4 January 2021

Available online 13 January 2021

#### Keywords:

Flavin

Isoalloxazine

Microwave synthesis

Chirality

Fluorescence

### ABSTRACT

We report the synthesis of new isoalloxazines using a microwave-assisted approach to make *N*-substituted-2-nitroanilines followed by one-pot reduction and condensation *via* Hemmerich's method. The influence of substituents on positions 7, 8, and 10 of flavin core on the optical properties is investigated. The aliphatic functionalities on N10 give rise to quantum yields of 0.7, while aromatic side-chains quench fluorescence. Relaxed geometries (DFT) of chiral and achiral derivatives have been used for TD-DFT calculations, which yielded good agreement with the experimental UV and CD data.

© 2021 Elsevier Ltd. All rights reserved.

## 1. Introduction

Flavins are coenzymes and photoreceptors that are ubiquitous in biotic systems, taking part in numerous biochemical transformations [1,2]. Representative examples of flavins are riboflavin (RF), flavin mononucleotide (FMN) and flavin adenine dinucleotide (FAD), which are prosthetic groups in flavoenzymes [3]. All these share a key structural feature that modulates their activity: the isoalloxazine core, which is a benzo[*g*]pteridine-2,4(3H)-dione able to accept one or two electrons (Fig. 1) [4]. The isoalloxazine is therefore one of the electroactive units within the biological environment and contributes to redox reactions, activation of oxygen, cell apoptosis, halogenation of aromatic substrates, respiratory electron transport chain, dehydrogenation of metabolites, DNA repair and many other [2,5,6].

Isoalloxazine-based flavins interact with cellular components through non-covalent interactions such as  $\pi$ - $\pi$  stacking, hydrogen bonds, electrostatic and charge-transfer interactions [5]. The side chain on the N10 position of isoalloxazine core (atom numbering is

given in Fig. 1) is responsible for the protein binding and specificity, while the rest of the substituents influence the stability, redox and acid-base properties as well as solubility [3]. The literature reports a plethora of experimental and theoretical studies on flavins and their interactions within biological environments [1,7,8]. However, these are highly complex systems with many interplaying components, making difficult to assess the binding mode, reactivity and properties of isoalloxazines. On this basis, synthetic flavin models have been designed to get insights into the cofactor-protein binding modes [9]. These models have opened up a new path towards development of artificial enzymes that mimic the behaviour of natural ones [10–12]. Most of flavin mimetics maintain the catalytically active isoalloxazine core but have been structurally modified to control their redox and photophysical properties.

The design of artificial enzymes based on flavins follows either the functionalisation of precursors or chemical modification and photodegradation of RF, FMN and FAD. The isoalloxazine core can be functionalised with small electron withdrawing or donating groups in any position [13–17] as well as with more complex groups. Examples of the latter include flavins functionalised with calixarenes [18], cyclophanes [19], fullerenes [20], fused macrocycles-isoalloxazine dyads [5,21] and flavin-peptide

\* Corresponding author.

E-mail address: [g.d.pantos@bath.ac.uk](mailto:g.d.pantos@bath.ac.uk) (G.D. Pantoș).

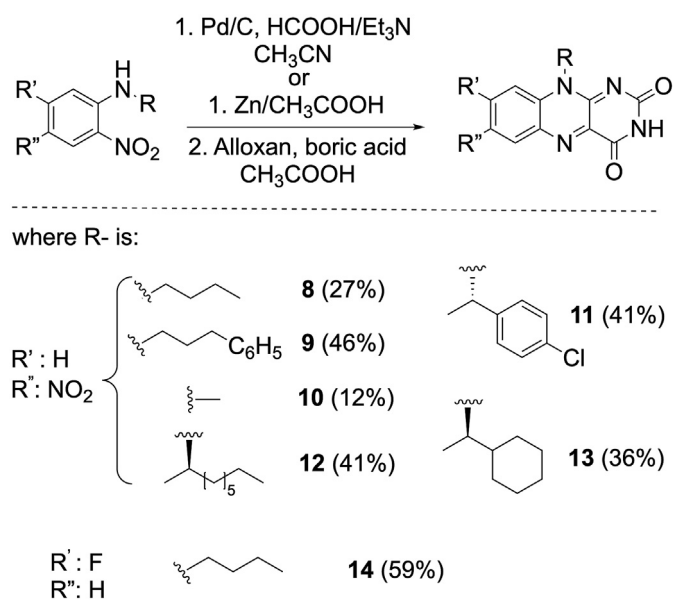


## 2.2. One-pot synthesis of isoalloxazines

The *N*-alkylated (di)nitroanilines **1–7** were reduced to the corresponding *o*-phenylenediamines followed by one-pot condensation with alloxan to form the isoalloxazines **8–14**. We have used the classical azeotropic mixture of formic acid-triethylamine (FA-Et<sub>3</sub>N) [33,34] and catalytic amounts of palladium on carbon (0.1 equiv) that generates hydrogen *in situ* for reduction of compounds **1, 2** and **4–7** (Scheme 2). This is a mild reducing system, which has allowed the chemoselective reduction of the nitro group in position 2, but not of that in position 4. Selectivity was achieved by cooling the system to  $-15\text{ }^{\circ}\text{C}$  and dropwise addition of FA. The benefit of FA-Et<sub>3</sub>N in the reduction process over other reducing agents is that the resulting carbon dioxide is thermodynamically stable, which makes the reaction irreversible [35]. Reduction of derivative **3** with just one nitro group was carried out in much stronger reducing environments (*i.e.* zinc powder and acetic acid; Scheme 2) following a protocol reported in the literature [36].

The catalysts used during reductions were filtered off and the crude mixtures were used immediately in the flavin formation. The isoalloxazine core was formed *via* Hemmerich's method [37], which involved the reaction of *N*-substituted *o*-phenylenediamines with alloxan in the presence of boric acid and acetic acid as solvent (Scheme 2). The condensation method is versatile, with shorter reaction times when performing the reaction at high temperatures ( $90\text{ }^{\circ}\text{C}$ ). The yield over the two steps (reduction and condensation) is higher if only one nitro group is present in the starting material (**14**). The substituents on the N10 position also influence the reaction progress, with the lowest yield over two steps being obtained for the methyl-substituted isoalloxazine **10** (12%). A possible explanation for this is the higher solubility of **10** in the reaction mixture. The one-step reduction/condensation method is versatile; however, for certain derivatives does not lead to isoalloxazine, but quinoxaline by-products [38].

Compounds **8** and **10** are reported in the literature [39], but no thorough characterisation is provided (only melting point and IR are reported). Literature reports ample information on flavins in general and other nitro- [9] and fluoro-substituted isoalloxazines



**Scheme 2.** One-pot reduction of *N*-alkylated (di)nitroanilines and condensation with alloxan to synthesise isoalloxazines **8–14**. The overall yields (over two steps) corresponding to each derivative are given in parentheses after product number.

[27,40]. The current work further expands the existent knowledge and tackles in detail the influence of substituents in positions 7, 8 and 10 on the (chiro)optical properties of synthetic isoalloxazines.

## 2.3. Photophysical properties of isoalloxazines **8–14**

The photophysical features of isoalloxazines **8–14** were investigated by means of absorption and fluorescence spectroscopies. The chiroptical properties of chiral derivatives **11–13** were explored using circular dichroism (CD). All measurements were carried out in acetonitrile.

The UV–Vis region of the absorption spectra of all isoalloxazines display similar pattern: a broad band around 425 nm flanked by two shoulders at 455 and 405 nm (Fig. 2A). This band arises from the lowest allowed  $\pi \rightarrow \pi^*$  transitions of isoalloxazine chromophore. This spectral feature is consistent with spectra of other flavin mimics in acetonitrile reported in the literature [41–44]. The rest of absorption profile has different characteristics depending on the substituent on the benzene ring of the flavin core (positions 7 and 8). The substituent on the N10 position does not significantly influence the absorption behaviour (all absorption spectra shown in Fig. S38). Therefore, all the nitro-isoalloxazines (**8–13**) show one large band around 295 nm and a weak one at 230 nm. A comparison between the 10-butyl-7-nitro (**8**) and 10-butyl-8-fluoro (**14**) derivatives is given in Fig. 2A. Flavin **14** displays a hypsochromically-shifted band compared to the nitro one: 265 vs 294 and another

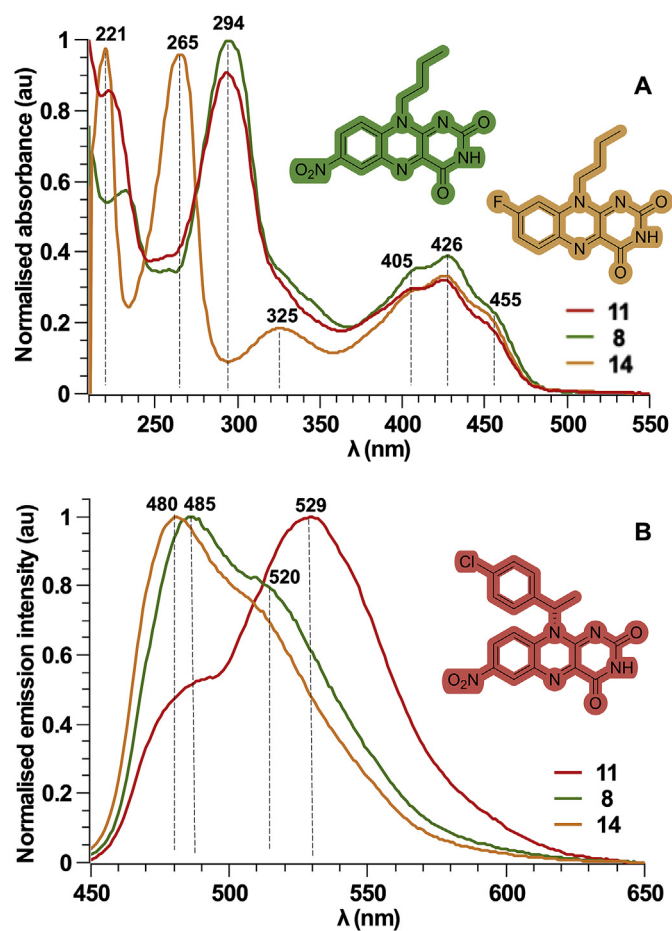


**Fig. 2.** A: Normalised absorption spectra of isoalloxazines **8** and **14** in acetonitrile. B: Normalised emission spectra of isoalloxazines **8, 14** and **11** in acetonitrile at 425 nm (**8** and **14**) and 426 nm (**11**) excitation wavelength.

band of similar amplitude around 220 nm (Fig. 2A). Literature data shows that strongly electron withdrawing functionalities (such as F<sub>3</sub>C-) in positions 7 or 8 [41] as well as substituents on the N3 position give rise to a band at 325 nm [43,44]. This explains the presence of the weaker band at 325 nm in the spectrum of fluoroisalloxazine **14**, which is not observed in the spectra of nitro derivatives (Fig. 2A).

The absorption profile across the UV–Vis region of biological flavins (e.g., RF) in acetonitrile is similar to that of our derivatives [45]. In terms of strength of isalloxazine chromophore, the synthetic flavins have larger molar extinction coefficients ( $\epsilon$ ) than RF ( $\epsilon_{\text{RF}} = 2100 \text{ L mol}^{-1} \text{ cm}^{-1}$  [46]), with 10-butyl-7-nitro flavin **8** being the strongest and the 10-methyl-7-nitro flavin **10** the weakest ( $12800 \text{ vs } 2670 \text{ L mol}^{-1} \text{ cm}^{-1}$ , respectively; Table 1; Fig. S42). These values are comparable to those of other synthetic isalloxazines recorded in the same solvent [44]. The  $\epsilon$  of derivatives **8–14** in acetonitrile are given in Table 1.

The fluorescence emission spectra of derivatives **8–10** and **12–14** in acetonitrile show similar spectral features (Figs. S41 and S42), with one broad band around 480 nm and a shoulder on its right centred at 520 nm (typical fluorescence emission spectra are shown in Fig. 2B). The emission band of nitro-derivatives **8**, **9** and **10** is shifted by 5 nm and that of **12** and **13** by 8 nm to longer wavelengths compared to the fluoro-substituted flavin **14**. This leads to slightly larger Stokes shifts for the nitro analogues. Fig. 2B compares the emission spectra of compounds **8** and **14**. Derivative **11** exhibits a different emission profile than the rest of isalloxazines in the series, with a broad band shifted at longer wavelengths (529 nm) and a shoulder on its right part (Fig. 2B).

The maximum wavelength from the emission spectra of each derivative and the corresponding Stokes shifts are summarised in Table 1. The emission spectral characteristics of compounds **8–14** are similar to those of other synthetic flavins reported in the literature [44]. The emission maximum has been attributed to S<sub>1</sub><sup>0</sup> → S<sub>0</sub><sup>0</sup> vibronic transition [47].

The fluorescence quantum yields ( $\Phi_{\text{FL}}$ ) of derivatives **8–14** in acetonitrile are provided in Table 1. All  $\Phi_{\text{FL}}$  were calculated using fluorescein as standard (we have used the  $\Phi_{\text{FL}}$  of fluorescein in ethanol as 0.79 [48]; details are given in the Experimental section). The substituents on the N10 position strongly influence the  $\Phi_{\text{FL}}$  of derivatives **8–14**, while the functionalities attached on the benzene ring of the flavin core do not affect it that much. Among the flavins in the series, the 10-methyl-7-nitro isalloxazine **10** has the highest  $\Phi_{\text{FL}}$  (0.71). This is followed closely by derivatives **8** and **14**, which have a butyl side-chain on the N10 position. The nitro (**8**) and fluoro (**14**) groups do not influence the  $\Phi_{\text{FL}}$ . The large  $\Phi_{\text{FL}}$  of these flavins indicate their low non-radiative decay rates [49]. To the best of our knowledge, these values are among the largest reported so far in the literature for synthetic isalloxazines. The  $\Phi_{\text{FL}}$  of biological

analogues are also much smaller compared to these ( $\Phi_{\text{FL}}$  of RF in acetonitrile is 0.47 [47]).

The  $\Phi_{\text{FL}}$  of derivatives **9** and **11–13** are lower compared to the alkyl-substituted flavins (Table 1). We associate this behaviour of **9** and **11** with fluorescence quenching processes induced by the aromatic units on these molecules. It is well-known that aromatics with organic donor or acceptor functionalities quench fluorescence in organic solvents through an electron transfer process [50]. The electron-acceptor nature of aromatic substituent in position N10 of compound **11** leads to a significant decrease down to 0.05, while the phenyl group on **9** induces a drop to 0.25. The higher  $\Phi_{\text{FL}}$  of **9** compared to **11** can be attributed to the position of the phenyl group relative to the isalloxazine core ( $\gamma$  vs  $\alpha$  in **11**) and different electronic properties. Derivatives **12** and **13** have a  $\Phi_{\text{FL}}$  of 0.31, suggesting that molecular crowding in the  $\alpha$  position relative to the flavin core lowers the  $\Phi_{\text{FL}}$ .

The chiroptical properties of chiral derivatives **11–13** have been

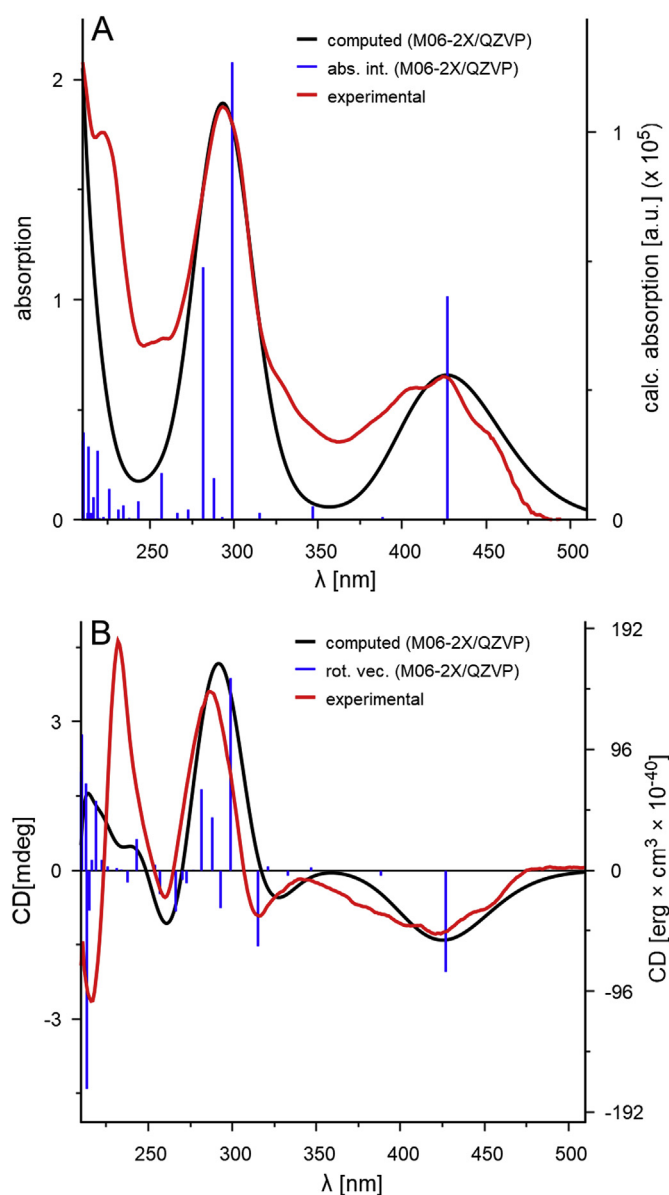


Fig. 3. Overlaid experimental ( $2 \times 10^{-4} \text{ M}$ ; red) and predicted (black) spectra of **11**. A: absorption and B: CD. The y axes on the left correspond to the experimental data, while those on the right to the predicted spectra.

Table 1  
Spectral characteristics of isalloxazines **8–14** shown in Scheme 2.

Product	Absorption		Emission		
	$\lambda_{\text{max}}$ (nm)	$\epsilon$ ( $\text{L mol}^{-1} \text{ cm}^{-1}$ )	$\lambda_{\text{max}}$ (nm)	Stokes shift (nm) <sup>a</sup>	$\Phi_{\text{FL}}$ <sup>b</sup>
<b>8</b>	425	$12800 \pm 0.1$	485	60	0.70
<b>9</b>	426	$4960 \pm 4.0$	486	60	0.25
<b>10</b>	426	$2670 \pm 0.3$	485	59	0.71
<b>11</b>	426	$4070 \pm 0.1$	529	103	0.05
<b>12</b>	428	$8950 \pm 0.9$	488	60	0.31
<b>13</b>	428	$2070 \pm 0.1$	488	60	0.31
<b>14</b>	425	$9860 \pm 0.6$	480	55	0.70

<sup>a</sup> The Stokes shifts were calculated as:  $\lambda_{\text{max}}$  emission –  $\lambda_{\text{max}}$  absorption (corresponding to the isalloxazine core).

<sup>b</sup> Fluorescence quantum yields at excitation wavelengths as  $\lambda_{\text{max}}$  in absorption spectra were calculated using fluorescein as standard.

explored by circular dichroism (CD). The CD spectrum of derivative **11** in acetonitrile is shown in Fig. 3 and provides valuable insights into optoelectronic and structural properties of this chiral flavin. The spectrum displays a negative Cotton effect centred at 425 nm, indicating that the chirality is transferred from the N10 substituent onto the intrinsically achiral isoalloxazine core. There are also two large positive bands around 290 and 230 nm. We have also performed variable temperature (VT) CD studies to assess if the chirality transfer is temperature dependant (Fig. S39). No significant modification was observed upon VT ramp (5–75 °C and return) apart from minor photodecomposition. Isoalloxazines **12** and **13** also have chiral centres in the  $\alpha$  position relative to the core as **11**. These bear a nonane-functionalised alkyl chain (**12**) or a cyclohexyl-based substituent (**13**) in position N10 instead of aromatic units. The CD spectra of **12** and **13** display a similar pattern to that of **11**, with the chiral information also being transferred onto the core. Their CD profile shows positive Cotton effects around 425 nm (Fig. S40). The literature reports some CD spectra of isoalloxazines, but most of them are on biological flavins, their modified analogues or flavinyl peptides. Therefore, no direct comparison of chiroptical properties could be done between our synthetic derivatives and previously reported examples.

In order to understand the optoelectronic properties of these synthetic flavins, we undertook (TD)DFT studies. The structures of derivatives **11–14** have been pre-optimised using semi empirical methods (PM7, convergence criterion 0.01 kcal/mol/Å) followed by DFT optimization using B3LYP-D3/6311+G\* theory level. The relaxed geometries of **11–14** obtained in the previous step were used in sTDDFT calculations for predicting the absorption (all) and CD (**11–13**) spectra. We have used hybrid-GGA (B3LYP), hybrid meta GGA (M06–2X, PW6B95) and range separated hybrid (CAM-B3LYP,  $\omega$ B97X,  $\omega$ B97X-D3) functionals with Pople style and Def2-Ahlrichs basis sets. Of the various combinations of functionals and basis sets used, M06–2X/QZVP/CH<sub>3</sub>CN gave the best results (compound **11**, Fig. 3A and B) with similarity factors of 0.96 (absorption, –1 nm shift) and 0.96 (CD, –7 nm shift) calculated using SpecDis [51] (for details see section 6 and Table S1 in the Supplementary material). These results allow us to lay the foundation for future pre-synthetic electronic/optical properties prediction of synthetic flavins.

### 3. Conclusion

We report herein an optimised method to synthesise a series of seven new isoalloxazines starting from commercially available (di)nitroanilines or dinitrohalobenzenes. The first step uses microwave irradiation to generate *N*-substituted-2-nitroanilines in good to quantitative yields via either S<sub>N</sub>2 or S<sub>N</sub>Ar mechanisms. The next step is the one-pot reduction of nitro groups to amines followed by condensation with alloxan to yield the isoalloxazines **8–14**. The optical properties (absorption/emission features, molar extinction coefficients, quantum yields) of all synthetic flavins in acetonitrile are discussed in detail. Three derivatives (**8**, **10**, **14**) in the series have large quantum yields of 0.7, while **9** and **11–13** undergo fluorescence quenching induced by aromatic units or bulky substituents in the  $\alpha$  position relative to the flavin core. The CD spectra of **11–13** show that the chiral information is efficiently transferred from the chiral substituent onto the isoalloxazine core. Predicted spectra using (TD)DFT calculations match well the experimental data. This work puts forward an optimised and versatile strategy to making synthetic flavins, which are important in model enzymatic studies as well as catalysis and as photoreceptors. The catalytic potential of all flavins reported in this work will be reported in due course.

## 4. Experimental section

### 4.1. Materials and methods

All reagents were purchased from commercial suppliers: Merck, Fisher, TCI and Fluorochem and used without further purification. <sup>1</sup>H and <sup>13</sup>C NMR spectra were recorded on 500 MHz Agilent Pro-pulse or 500 MHz Bruker Avance II+ (<sup>1</sup>H at 500 MHz, <sup>13</sup>C at 126 MHz) instruments, as stated. Chemical shifts ( $\delta$ ) are reported in parts per million (ppm). Coupling constants (*J*) are reported in Hertz (Hz), and signal multiplicity is denoted as broad singlet (br s), singlet (s), doublet (d), doublet of doublets (dd), triplet (t), quartet (q), pentet (p), sextet (sext), doublet of doublets of doublets (ddd), doublet of triplets (dt), triplet of doublets (td) and multiplet (m). Samples for NMR spectroscopy were prepared with CDCl<sub>3</sub>, acetone-*d*<sub>6</sub> or DMSO-*d*<sub>6</sub> as stated in each case. All spectra were acquired at 25 °C and were referenced to the residual solvent peaks. The <sup>1</sup>H and <sup>13</sup>C NMR spectra (Figs. S1–28) contain small traces of water, dichloromethane, acetone, ethyl acetate and petroleum ether 40–60%. Electrospray ionisation quadrupole time-of-flight (ESI-Q-TOF) mass spectrometry was performed on an Agilent Technologies 6545 Q-TOF LC-MS instrument using a positive- or negative-ion mode as stated in each case (Figs. S29–37). Microwave-assisted reactions were conducted in a CEM Discover microwave reactor using a sealed reaction vessel.

CD and absorption experiments (Figs. S38–41) were performed in acetonitrile on an Applied Photophysics Chirascan Circular Dichroism Spectrophotometer equipped with a Peltier temperature controller using a 1 cm pathlength quartz cuvette. The background corresponding to the acetonitrile and cuvette's absorption was subtracted from subsequent measurements. The following parameters were used: wavelength range 210–550 nm, time-per-point 1 s, monochromator bandwidth 1 nm, temperature 20 °C. Fluorescence spectra (Figs. S42–43) were recorded in acetonitrile using a 1 cm fluorescence quartz cuvette on an Applied Photophysics Chirascan Circular Dichroism Spectrophotometer equipped with a CS/SEM accessory. The following parameters were used: wavelength range 440–650 nm (emission spectra) and 210–550 nm (excitation spectra), time-per-point 0.5 s, monochromator bandwidth 2 nm, slit width 1 mm (bandpass 4.65 nm), PMU 1000 V, temperature 20 °C. The excitation and emission wavelengths used in each case are given in the Supplementary material. The quantum yields of compounds **8–14** were calculated using fluorescein in ethanol (0.79) as reference and 1.36 and 1.344 the refractive indices of ethanol and acetonitrile, respectively.

Molecular modelling studies were carried out using PM7 (MOPAC2016) [52] for pre-optimizing the structures followed by DFT geometry optimization using B3LYP-D3/6311+G\*. The TD-DFT studies were performed at various functionals with 6311++G\*\* or QZPT basis sets using, where appropriate, D3 dispersion correction and an acetonitrile CPCM solvent model. All DFT calculation were performed using ORCA v. 4.2.1 [53] with Gabedit v. 2.5.0 [54] as GUI (further information is provided in the Supplementary material, Table S1, Fig. S44). The predicted UV–vis and CD spectra were constructed in SpecDis by fitting Gaussian curves over the oscillator strength (UV–vis) and rotational strength (CD) computed with the sTDDFT (M06–2X/QZVP/CH<sub>3</sub>CN). The exponential half-width for the Gaussian fit ranged between 0.25 and 0.30 eV as obtained from similarity factor calculations implemented SpecDis.

### 4.2. General procedure A to synthesise compounds 1–3

A 10-mL microwave tube was charged with 2,4-dinitroaniline (100 mg, 0.546 mmol, 1 equiv) for derivatives **1** and **2** or 5-fluoro-2-nitroaniline (100 mg, 0.640 mmol, 1 equiv) for derivative

**3** and acetonitrile (5 mL). The microwave tube was placed on a stirrer plate and sodium hydride 60% suspension in mineral oil (2 equiv) was added. The yellow solution turned deep red upon sodium hydride addition. The reaction mixture was stirred 5 min on bench and the corresponding alkylating reagent was added (2 equiv). The microwave tube was placed in a microwave reactor and the reaction mixture was heated for 3 h at 120 °C under microwave irradiation (at 150 W). The solvent was removed under reduced pressure to yield a red-brown residue, which was re-dissolved in water (150 mL). The pH of the solution was adjusted to 2 using 1 M HCl<sub>aq</sub>. The solution was extracted with ethyl acetate (2 × 100 mL). The collected organic fractions were washed with brine (3 × 100 mL), dried over anhydrous magnesium sulfate and solvent removed under reduced pressure to obtain a yellow solid. The product was purified by flash column chromatography using silica as stationary phase (60 Å particle size). The solvents were removed under reduced pressure and the solid dried *in vacuo* to yield the corresponding alkylated amine.

#### 4.2.1. *N*-butyl-2,4-dinitroaniline (**1**)

Started with 1-bromobutane (149.6 mg, 118 μL, 1.092 mmol) and sodium hydride (26.2 mg, 1.092 mmol). Purified by column chromatography (CH<sub>2</sub>Cl<sub>2</sub>:petroleum ether 1:1, v/v ratio), product collected as second fraction. Yellow solid, 94.2 mg, 0.394 mmol, 72%. <sup>1</sup>H NMR (500 MHz, CDCl<sub>3</sub>) δ 9.14 (d, *J* = 2.7 Hz, 1H), 8.55 (br s, 1H), 8.27 (dd, *J* = 9.5, 2.7 Hz, 1H), 6.92 (d, *J* = 9.5 Hz, 1H), 3.41 (td, *J* = 7.1, 5.3 Hz, 2H), 1.77 (p, *J* = 7.3 Hz, 2H), 1.50 (dt, *J* = 14.8, 7.4 Hz, 2H), 1.01 (t, *J* = 7.4 Hz, 3H). The <sup>1</sup>H NMR data matches the one reported in the literature [29].

#### 4.2.2. 2,4-dinitro-*N*-(3-phenylpropyl)aniline (**2**)

Started with 1-bromo-3-phenylpropane (218 mg, 1.092 mmol) and sodium hydride (26.2 mg, 1.092 mmol). Purified by column chromatography (CH<sub>2</sub>Cl<sub>2</sub>:petroleum ether 1:1, v/v ratio), product collected as second fraction. Yellow solid, 132 mg, 0.438 mmol, 80%. <sup>1</sup>H NMR (500 MHz, CDCl<sub>3</sub>) δ 9.11 (d, *J* = 2.6 Hz, 1H), 8.59 (t, *J* = 5.6 Hz, 1H), 8.24 (dd, *J* = 9.5, 2.6 Hz, 1H), 7.38–7.29 (m, 2H), 7.27–7.17 (m, 3H), 6.86 (d, *J* = 9.5 Hz, 1H), 3.45 (q, *J* = 5.6 Hz, 2H), 2.83 (t, *J* = 7.4 Hz, 2H), 2.15 (p, *J* = 7.3 Hz, 2H).

#### 4.2.3. *N*-butyl-5-fluoro-2-nitroaniline (**3**)

Started with 1-bromobutane (175.5 mg, 138 μL, 1.281 mmol) and sodium hydride (30.7 mg, 1.281 mmol). Purified by column chromatography (CH<sub>2</sub>Cl<sub>2</sub>:petroleum ether 1:1, v/v ratio), product collected as first fraction. Yellow solid, 55.1 mg, 0.259 mmol, 41%. <sup>1</sup>H NMR (500 MHz, CDCl<sub>3</sub>) δ 8.20 (dd, *J* = 9.5, 6.1 Hz, 1H), 8.16 (br s, 1H), 6.48 (dd, *J* = 11.5, 2.6 Hz, 1H), 6.34 (ddd, *J* = 9.5, 7.2, 2.6 Hz, 1H), 3.25 (td, *J* = 7.1, 5.1 Hz, 2H), 1.72 (p, *J* = 7.3 Hz, 2H), 1.49 (sext, *J* = 7.4 Hz, 2H), 1.00 (t, *J* = 7.4 Hz, 3H). <sup>13</sup>C NMR (126 MHz, CDCl<sub>3</sub>) δ 168.59, 166.55, 147.58 (d, *J* = 13.7 Hz), 129.96 (d, *J* = 12.4 Hz), 128.71, 103.72 (d, *J* = 24.8 Hz), 99.20 (d, *J* = 26.9 Hz), 30.74, 20.19, 13.71.

### 4.3. Synthesis of compound **4**

The reaction protocol was modified from Ref. [33]. A 250-mL round-bottomed flask was charged with 1-chloro-2,4-dinitrobenzene (4 g, 19.748 mmol, 1 equiv) and ethanol (150 mL) was added. The solution was stirred 15 min at room temperature, then methylamine (40% w/w solution in water; 1.23 g, 1.75 mL, 39.496 mmol, 2 equiv) was added (a precipitate started to form). The reaction mixture was stirred at room temperature for 1 h and the precipitate formed was filtered off, washed with a small amount of ethanol and dried *in vacuo*.

#### 4.3.1. *N*-methyl-2,4-dinitroaniline (**4**)

Yellow solid (3.9 g, 19.748 mmol, quant.). <sup>1</sup>H NMR (500 MHz, acetone-*d*<sub>6</sub>) δ 9.01 (d, *J* = 2.7 Hz, 1H), 8.82 (br s, 1H), 8.35 (dd, *J* = 9.6, 2.7 Hz, 1H), 7.25 (d, *J* = 9.6 Hz, 1H), 3.25 (d, *J* = 5.1 Hz, 3H). The <sup>1</sup>H NMR data matches the one reported in the literature [33].

### 4.4. General procedure **B** to synthesise compounds **5–7**

A 10-mL microwave tube was charged with 1-chloro-2,4-dinitrobenzene (200 mg, 0.987 mmol, 1 equiv) and absolute ethanol (5 mL). To this, the relevant primary amine (2 equiv) was added and the reaction mixture was heated for 10 min at 140 °C under microwave irradiation (at 300 W). The solvent was removed under reduced pressure to give an orange residue. Product **5** was purified by flash column chromatography using silica as stationary phase (60 Å particle size). The crude residue obtained after solvent evaporation in the case of derivatives **6** and **7** was re-dissolved in dichloromethane (50 mL) and extracted with saturated NaHCO<sub>3</sub> (3 × 50 mL) and 1 × 100 mL saturated NaCl. The collected organic fractions were dried over anhydrous magnesium sulfate and the solvent removed under reduced pressure. The excess of unreacted amine was removed under high vacuum to yield the corresponding alkylated amines.

#### 4.4.1. (*S*)-*N*-(1-(4-chlorophenyl)ethyl)-2,4-dinitroaniline (**5**)

Started with (*S*)-4-chloro- $\alpha$ -methylbenzylamine (307.3 mg, 1.975 mmol) Purified by column chromatography (CH<sub>2</sub>Cl<sub>2</sub>:petroleum ether 1:1, v/v ratio), product collected as third fraction. Yellow solid (206 mg, 0.641 mmol, 65%). <sup>1</sup>H NMR (500 MHz, CDCl<sub>3</sub>) δ 9.11 (d, *J* = 2.7 Hz, 1H), 8.86 (d, *J* = 5.9 Hz, 1H), 8.12 (dd, *J* = 9.5, 2.7 Hz, 1H), 7.36 (d, *J* = 8.3 Hz, 2H), 7.29 (d, *J* = 8.3 Hz, 2H), 6.72 (d, *J* = 9.5 Hz, 1H), 4.80 (p, *J* = 6.6 Hz, 1H), 1.73 (d, *J* = 6.6 Hz, 3H). <sup>13</sup>C NMR (126 MHz, CDCl<sub>3</sub>) δ 147.3, 140.5, 136.5, 133.8, 130.8, 130.1, 129.5, 126.9, 124.0, 115.2, 53.3, 24.6. HRMS *m/z* calculated for C<sub>14</sub>H<sub>12</sub>ClN<sub>3</sub>O<sub>4</sub>: [M – H]<sup>–</sup> 320.0444, found: 320.0445.

#### 4.4.2. (*R*)-2,4-dinitro-*N*-(nonan-2-yl)aniline (**6**)

Started with (*R*)-2-aminononane (283.0 mg, 362 μL, 1.975 mmol). Purified by extraction with NaHCO<sub>3</sub>(sat) and NaCl(sat) followed by the excess amine removal under reduced pressure. Orange viscous oil, 305.1 mg, 0.987 mmol, quantitative. <sup>1</sup>H NMR (500 MHz, CDCl<sub>3</sub>) δ 9.15 (d, *J* = 2.7 Hz, 1H), 8.53 (d, *J* = 7.8 Hz, 1H), 8.25 (dd, *J* = 9.6, 2.7 Hz, 1H), 6.91 (d, *J* = 9.6 Hz, 1H), 3.78 (p, *J* = 6.6 Hz, 1H), 1.76–1.58 (m, 2H), 1.46–1.36 (m, 2H), 1.34 (d, *J* = 6.4 Hz, 4H), 1.33–1.24 (m, 6H), 0.88 (t, *J* = 6.8 Hz, 4H). <sup>13</sup>C NMR (126 MHz, CDCl<sub>3</sub>) δ 147.8, 130.3, 124.7, 114.0, 77.3, 77.0, 76.7, 49.3, 36.6, 31.7, 29.4, 29.1, 25.9, 22.6, 20.4, 14.1. HRMS *m/z* calculated for C<sub>15</sub>H<sub>23</sub>N<sub>3</sub>O<sub>4</sub>: [M – H]<sup>–</sup> 308.1616, found: 308.1615.

#### 4.4.3. (*R*)-*N*-(1-cyclohexylethyl)-2,4-dinitroaniline (**7**)

Started with (*R*)-1-cyclohexylethylamine (251.1 mg, 290 μL, 1.975 mmol). Purified by extraction with NaHCO<sub>3</sub>(sat) and NaCl(sat) followed by the excess amine removal under reduced pressure. Orange viscous oil, 289.3 mg, 0.987 mmol, quantitative. <sup>1</sup>H NMR (500 MHz, CDCl<sub>3</sub>) δ 9.15 (d, *J* = 2.7 Hz, 1H), 8.67 (s, 1H), 8.23 (ddd, *J* = 9.7, 2.8, 0.8 Hz, 1H), 6.92 (d, *J* = 9.6 Hz, 1H), 3.70–3.60 (m, 1H), 1.89–1.67 (m, 7H), 1.57 (tdt, *J* = 8.7, 5.7, 2.8 Hz, 2H), 1.28–1.19 (m, 2H), 1.19–1.03 (m, 3H). <sup>13</sup>C NMR (126 MHz, CDCl<sub>3</sub>) δ 148.2, 130.5, 124.9, 114.2, 54.1, 43.2, 29.4, 29.0, 26.4, 26.3, 26.2, 17.5. HRMS *m/z* calculated for C<sub>14</sub>H<sub>19</sub>N<sub>3</sub>O<sub>4</sub>: [M – H]<sup>–</sup> 292.1303, found: 292.1302.

#### 4.5. General procedure to synthesise compounds **8–13**

The two-step synthesis of isoalloxazines **8–13** from precursors **1, 2, 4–7** was performed in one-pot: reduction of corresponding alkylated amines followed by immediate coupling. The reduction protocol was modified from Ref. [33], and the coupling method was modified from Ref. [37]. Both steps are sensitive to light, therefore the reaction vessels were covered in aluminium foil and exposure to light was minimised during work-up.

A 50-mL two-necked round-bottomed flask was charged with the corresponding alkylated aniline (1 equiv) suspended in dry acetonitrile (1.35 mL/mmol alkylated amine). The flask was placed under nitrogen atmosphere and dry triethylamine (Et<sub>3</sub>N; 4.7 equiv) was added. Palladium on carbon (Pd/C, 10 wt%; 0.1 equiv) was added. The reaction mixture was cooled to –15 °C using a mixture of sodium chloride:ice in 1:3 w/w ratio. While in the cooling bath, a freshly prepared solution of formic acid (FA; 4.8 equiv) in dry acetonitrile (1.35 mL/mmol alkylated aniline) was added dropwise to the reaction mixture. The cooling bath was removed and the reaction mixture was refluxed (at 80–85 °C) for 3 h under nitrogen atmosphere. The suspension colour changed during the reaction from yellow to orange, green and lastly to red. After 3 h, the reaction mixture was cooled down and the Pd/C was quickly filtered off through a pad of Celite® using a sintered funnel and suction. For compounds **8, 9, 10, 12** and **13**: the Celite® was washed with glacial acetic acid (5 mL). To the red-coloured solution, a mixture of alloxan monohydrate (1.5 equiv) and boric acid (1.5 equiv) dissolved in hot glacial acetic acid (10 mL) was added and the reaction mixture was stirred overnight at room temperature under nitrogen atmosphere. For compound **11**: the Celite® was washed with glacial acetic acid (15 mL) and alloxan monohydrate (1.5 equiv) and boric acid (1.5 equiv) were added as solids. The reaction mixture was heated for 1 h at 90 °C under nitrogen atmosphere. In all cases: the solvent was removed under reduced pressure to yield a dark red viscous oil. The product was purified by column chromatography (except compound **10**) using silica as stationary phase (60 Å particle size). The solvents were removed under reduced pressure and the solid dried *in vacuo* to yield the corresponding isoalloxazine.

##### 4.5.1. 10-butyl-7-nitrobenzo[g]pteridine-2,4(3H,10H)-dione (**8**)

Started with compound **1** (294 mg, 1.406 mmol), Pd/C (15.6 mg, 0.146 mmol), Et<sub>3</sub>N (959 μL, 6.880 mmol) and FA (265 μL, 7.027 mmol). For second step: alloxan monohydrate (337.6 mg, 2.109 mmol) and boric acid (130.4 mg, 2.109 mmol). Purified by column chromatography (CH<sub>2</sub>Cl<sub>2</sub>:acetone 9:1, v/v ratio) as second fraction. Yellow solid, 119 mg, 0.376 mmol, 27% over two steps. <sup>1</sup>H NMR (500 MHz, DMSO-*d*<sub>6</sub>) δ 11.60 (br s, 1H), 8.85 (d, *J* = 2.7 Hz, 1H), 8.61 (dd, *J* = 9.4, 2.7 Hz, 1H), 8.14 (d, *J* = 9.4 Hz, 1H), 4.58 (t, *J* = 7.4 Hz, 2H), 1.70 (p, *J* = 7.9 Hz, 2H), 1.49 (sext, *J* = 7.5 Hz, 2H), 0.97 (t, *J* = 7.4 Hz, 3H). <sup>13</sup>C NMR (126 MHz, DMSO-*d*<sub>6</sub>) δ 159.6, 156.0, 151.5, 144.3, 141.7, 137.2, 134.0, 128.3, 127.2, 118.2, 44.93, 28.9, 19.9, 14.2. HRMS *m/z* calculated for C<sub>14</sub>H<sub>13</sub>N<sub>5</sub>O<sub>4</sub>: [M+Na]<sup>+</sup> 338.0860, found: 338.0857.

##### 4.5.2. 7-nitro-10-(3-phenylpropyl)benzo[g]pteridine-2,4(3H,10H)-dione (**9**)

Started with compound **2** (119 mg, 0.395 mmol), Pd/C (4.7 mg, 0.044 mmol), Et<sub>3</sub>N (290 μL, 2.061 mmol) and FA (79 μL, 2.105 mmol). For second step: alloxan monohydrate (94.8 mg, 0.592 mmol) and boric acid (36.6 mg, 0.592 mmol). Purified by column chromatography (CH<sub>2</sub>Cl<sub>2</sub>:acetone 9:1, v/v ratio) as second fraction. Dark orange solid, 75 mg, 0.199 mmol, 46% over two steps.

<sup>1</sup>H NMR (500 MHz, DMSO-*d*<sub>6</sub>) δ 11.62 (br s, 1H), 8.84 (d, *J* = 2.7 Hz, 1H), 8.59 (dd, *J* = 9.4, 2.7 Hz, 1H), 8.11 (d, *J* = 9.4 Hz, 1H), 7.32–7.20 (m, 4H), 7.21–7.16 (m, 1H), 4.66 (t, *J* = 7.7 Hz, 2H), 2.84–2.78 (m, 2H), 2.05 (t, *J* = 7.8 Hz, 2H). <sup>13</sup>C NMR (126 MHz, DMSO-*d*<sub>6</sub>) δ 171.2, 159.6, 156.0, 151.6, 144.3, 141.4, 137.2, 134.0, 128.8, 128.6, 128.3, 127.2, 126.4, 44.9, 32.5, 28.4. HRMS *m/z* calculated for C<sub>19</sub>H<sub>15</sub>N<sub>5</sub>O<sub>4</sub>: [M+H]<sup>+</sup> 378.1197, found: 378.1202.

##### 4.5.3. 10-methyl-7-nitrobenzo[g]pteridine-2,4(3H,10H)-dione (**10**)

Started with compound **4** (500 mg, 2.536 mmol), Pd/C (27.6 mg, 0.259 mmol), Et<sub>3</sub>N (1650 μL, 11.838 mmol) and FA (460 μL, 12.192 mmol). For second step: alloxan monohydrate (302.5 mg, 1.890 mmol) and boric acid (116.8 mg, 1.890 mmol). The precipitate formed over time was filtered off, washed with diethyl ether (100 mL) and dried *in vacuo*. Orange solid, 78 mg, 0.284 mmol, 12% over two steps. <sup>1</sup>H NMR (500 MHz, DMSO-*d*<sub>6</sub>) δ 11.61 (s, 1H), 8.85 (d, *J* = 2.7 Hz, 1H), 8.64 (dd, *J* = 9.4, 2.7 Hz, 1H), 8.11 (d, *J* = 9.4 Hz, 1H), 3.99 (s, 3H). <sup>13</sup>C NMR (126 MHz, DMSO-*d*<sub>6</sub>) δ 159.6, 155.8, 151.9, 144.5, 141.6, 138.0, 133.7, 128.4, 127.0, 118.4, 32.8. HRMS *m/z* calculated for C<sub>11</sub>H<sub>7</sub>N<sub>5</sub>O<sub>4</sub>: [M+H]<sup>+</sup> 274.0571, found: 274.0570.

##### 4.5.4. (S)-10-(1-(4-chlorophenyl)ethyl)-7-nitrobenzo[g]pteridine-2,4(3H,10H)-dione (**11**)

Started with compound **5** (100 mg, 0.311 mmol), Pd/C (3.3 mg, 0.031 mmol), Et<sub>3</sub>N (204 μL, 1.464 mmol) and FA (57 μL, 1.495 mmol). For second step: alloxan monohydrate (74.8 mg, 0.467 mmol) and boric acid (28.9 mg, 0.467 mmol). Purified by column chromatography (CH<sub>2</sub>Cl<sub>2</sub>:acetone 9:1, v/v ratio) as fourth fraction. Dark orange-red solid, 50 mg, 0.126 mmol, 41% over two steps. <sup>1</sup>H NMR (500 MHz, CDCl<sub>3</sub>) δ 9.13 (d, *J* = 2.7 Hz, 1H), 8.58 (br s, 1H), 8.35 (dd, *J* = 9.5, 2.7 Hz, 1H), 7.69 (d, *J* = 7.4 Hz, 1H), 7.46 (d, *J* = 9.5 Hz, 1H), 7.39 (d, *J* = 7.4 Hz, 2H), 7.22–7.17 (m, 2H), 2.06 (d, *J* = 7.2 Hz, 3H). <sup>13</sup>C NMR (126 MHz, acetone-*d*<sub>6</sub>) δ 158.5, 152.5, 144.1, 141.5, 137.4, 135.0, 133.1, 129.0, 128.0, 127.4, 127.0, 119.2, 53.4, 15.0.

##### 4.5.5. (R)-7-nitro-10-(nonan-2-yl)benzo[g]pteridine-2,4(3H,10H)-dione (**12**)

Started with compound **6** (100 mg, 0.323 mmol), Pd/C (3.4 mg, 0.032 mmol), Et<sub>3</sub>N (212 μL, 1.520 mmol) and FA (58.6 μL, 1.552 mmol). For second step: alloxan monohydrate (77.7 mg, 0.485 mmol) and boric acid (29.9 mg, 0.485 mmol). Purified by column chromatography (CH<sub>2</sub>Cl<sub>2</sub>:acetone 9:1, v/v ratio) as fourth fraction. A second purification was performed on this fraction using (CH<sub>2</sub>Cl<sub>2</sub>:petroleum ether 9:1, v/v ratio). The dark orange-red solid was collected as the fourth fraction, 50 mg, 0.126 mmol, 41% over two steps. <sup>1</sup>H NMR (500 MHz, CDCl<sub>3</sub>) δ 9.50 (s, 1H), 9.12 (d, *J* = 2.6 Hz, 1H), 8.61 (d, *J* = 8.9 Hz, 1H), 8.07 (d, *J* = 9.5 Hz, 1H), 6.53 (q, *J* = 7.6 Hz, 1H), 2.11 (d, *J* = 9.2 Hz, 2H), 1.74 (d, *J* = 7.2 Hz, 3H), 1.22 (dqt, *J* = 13.8, 10.2, 6.0 Hz, 10H), 0.83 (t, *J* = 6.9 Hz, 3H). <sup>13</sup>C NMR (126 MHz, CDCl<sub>3</sub>) δ 158.2, 154.9, 151.8, 144.5, 139.6, 136.0, 135.0, 129.1, 128.0, 118.1, 54.4, 34.6, 31.6, 29.2, 28.9, 26.9, 22.5, 18.5, 14.0. HRMS *m/z* calculated for C<sub>19</sub>H<sub>23</sub>N<sub>5</sub>O<sub>4</sub>: [M+H]<sup>+</sup> 386.1823, found: 386.1824.

##### 4.5.6. (R)-10-(1-cyclohexylethyl)-7-nitrobenzo[g]pteridine-2,4(3H,10H)-dione (**13**)

Started with compound **7** (100 mg, 0.341 mmol), Pd/C (3.6 mg, 0.034 mmol), Et<sub>3</sub>N (224 μL, 1.603 mmol) and FA (61.8 μL, 1.637 mmol). For second step: alloxan monohydrate (81.9 mg, 0.512 mmol) and boric acid (31.6 mg, 0.512 mmol). Purified by column chromatography (CH<sub>2</sub>Cl<sub>2</sub>:acetone 9:1, v/v ratio) as fourth fraction. A second purification was performed on this fraction using

(CH<sub>2</sub>Cl<sub>2</sub>:petroleum ether 9:1, v/v ratio). The dark orange-red solid was collected as the second fraction, 47 mg, 0.123 mmol, 36% over two steps. <sup>1</sup>H NMR (400 MHz, CDCl<sub>3</sub>) δ 9.08 (d, *J* = 2.7 Hz, 1H), 9.02 (s, 1H), 8.54 (dd, *J* = 9.6, 2.7 Hz, 1H), 8.00 (d, *J* = 9.6 Hz, 1H), 6.22 (dq, *J* = 11.2, 7.2 Hz, 1H), 2.23–2.13 (m, 1H), 2.02 (d, *J* = 9.6 Hz, 2H), 1.79 (d, *J* = 6.7 Hz, 1H), 1.65 (d, *J* = 7.2 Hz, 3H), 1.63–1.56 (m, 4H), 1.24–1.20 (m, 1H), 1.01–0.95 (m, 2H). <sup>13</sup>C NMR (101 MHz, CDCl<sub>3</sub>) δ 158.3, 154.8, 152.3, 144.8, 139.8, 136.3, 135.1, 129.3, 128.2, 118.3, 77.5, 77.2, 76.8, 59.1, 41.4, 30.9, 29.5, 25.6, 16.9. HRMS *m/z* calculated for C<sub>18</sub>H<sub>19</sub>N<sub>5</sub>O<sub>4</sub>: [M+H]<sup>+</sup> 370.1510, found: 370.1510.

#### 4.6. Synthesis of compound 14

The reaction protocol was modified from Refs. [36,55]. A 50-mL round-bottomed flask was charged with compound 14 (55 mg, 0.259 mmol, 1 equiv) and glacial acetic acid (2.5 mL) and the flask was placed under nitrogen atmosphere. Zinc dust (170 mg, 2.598 mmol, 10 equiv) was added in portions over 3 min. The temperature of the reaction was maintained below 40 °C using a cold water bath. The reaction mixture was stirred 30 min at room temperature, after which the catalyst was filtered off through a pad of Celite® using a sintered funnel and suction. The Celite® was washed with glacial acetic acid (5 mL). Alloxan monohydrate (48.7 mg, 0.304 mmol, 1.2 equiv) and boric acid (24.4 mg, 0.395 mmol, 1.5 equiv) were added to the obtained diamine solution. The reaction mixture was heated for 1 h at 90 °C under nitrogen atmosphere. The solvent was removed under reduced pressure to obtain a dark red viscous oil. The flask was covered in aluminium foil during the reactions.

##### 4.6.1. 10-butyl-8-fluorobenzo[*g*]pteridine-2,4(3*H*,10*H*)-dione (14)

Purified by column chromatography (CH<sub>2</sub>Cl<sub>2</sub>:acetone 9:1, v/v ratio) as second fraction. Yellow solid, 44 mg, 0.153 mmol, 59%. <sup>1</sup>H NMR (500 MHz, Acetone-*d*<sub>6</sub>) δ 8.22 (dd, *J* = 8.6, 6.1 Hz, 1H), 7.79 (dd, *J* = 10.7, 2.5 Hz, 1H), 7.50 (td, *J* = 8.6, 2.5 Hz, 1H), 4.70 (t, *J* = 8.0 Hz, 2H), 1.87 (p, *J* = 7.7 Hz, 2H), 1.57 (dt, *J* = 15.0, 7.5 Hz, 2H), 1.02 (t, *J* = 7.4 Hz, 3H). <sup>13</sup>C NMR (126 MHz, DMSO-*d*<sub>6</sub>) δ 160.1, 156.1, 151.0, 138.4, 135.1 (d, *J* = 11.2 Hz), 134.7, 132.5, 115.2 (d, *J* = 24.5 Hz), 103.4 (d, *J* = 28.6 Hz), 44.9, 28.8, 19.9, 14.2. HRMS *m/z* calculated for C<sub>14</sub>H<sub>13</sub>FN<sub>4</sub>O<sub>2</sub>: [M+H]<sup>+</sup> 289.1095, found: 289.1097.

#### Declaration of competing interest

The authors declare that they have no known competing financial interests or personal relationships that could have appeared to influence the work reported in this paper

#### Acknowledgments

This paper is a contribution to special issue in memory of Prof. Jon Williams. An excellent colleague and chemist, he was a strong presence in our department who is sorely missed.

The authors gratefully acknowledge an EPSRC DTP (to D.M.R.) and the University of Bath for a visiting PhD researcher position (T.M.) which was also supported by Japan Student Services Organization (JASSO).

#### Appendix A. Supplementary data

Supplementary data to this article can be found online at <https://doi.org/10.1016/j.tet.2021.131925>.

#### References

- [1] A.M. Edwards, in: E. Silva, A.M. Edwards (Eds.), *Compr. Ser. Photochem. Photobiol. Sci.*, Royal Society of Chemistry, Cambridge, 2007, pp. 1–11.
- [2] J. Richtar, P. Heinrichova, D. Apaydin, V. Schmiedova, C. Yumusak, A. Kovalenko, M. Weiter, N. Sariciftci, J. Krajcovic, *Molecules* 23 (2018) 2271.
- [3] A. Kormányos, M.S. Hossain, G. Ghadimkhani, J.J. Johnson, C. Janáky, N.R. de Tacconi, F.W. Foss, Y. Paz, K. Rajeshwar, *Chem. Eur. J.* 22 (2016) 9209–9217.
- [4] W. Kaim, B. Schwederski, O. Heilmann, F.M. Hornung, *Coord. Chem. Rev.* 182 (1999) 323–342.
- [5] A. Farrán, J. Mohanraj, G.J. Clarkson, R.M. Claramunt, F. Herranz, G. Accorsi, *Photochem. Photobiol. Sci.* 12 (2013) 813.
- [6] P. Ménová, V. Eigner, J. Čejka, H. Dvořáková, M. Šanda, R. Cibulka, *J. Mol. Struct.* 1004 (2011) 178–187.
- [7] S. Weber, E. Schleicher (Eds.), *Flavins and Flavoproteins*, Springer, New York, New York, NY, 2014.
- [8] S.K. Chapman, G.A. Reid (Eds.), *Flavoprotein Protocols*, Humana Press, Totowa, NJ, 1999.
- [9] S.T. Caldwell, L.J. Farrugia, S.G. Hewage, N. Kryvokhyzha, V.M. Rotello, G. Cooke, *Chem. Commun.* (2009) 1350.
- [10] Y. Murakami, J. Kikuchi, Y. Hisaeda, O. Hayashida, *Chem. Rev.* 96 (1996) 721–758.
- [11] J.T. Slama, C. Radziejewski, S. Oruganti, E.T. Kaiser, *J. Am. Chem. Soc.* 106 (1984) 6778–6785.
- [12] S. Ghisla, V. Massey, *Biochem. J.* 239 (1986) 1–12.
- [13] B.J. Marsh, D.R. Carbery, *Tetrahedron Lett.* 51 (2010) 2362–2365.
- [14] S. Chen, M.S. Hossain, F.W. Foss, *Org. Lett.* 14 (2012) 2806–2809.
- [15] A.T. Murray, J.D. Challinor, C.E. Gulácsy, C. Lujan, L.E. Hatcher, C.R. Pudney, P.R. Raithby, M.P. John, D.R. Carbery, *Org. Biomol. Chem.* 14 (2016) 3787–3792.
- [16] A.T. Murray, P. Matton, N.W.G. Fairhurst, M.P. John, D.R. Carbery, *Org. Lett.* 14 (2012) 3656–3659.
- [17] Y.-M. Legrand, M. Gray, G. Cooke, V.M. Rotello, *J. Am. Chem. Soc.* 125 (2003) 15789–15795.
- [18] S. Sayin, G. Uysal Akkuş, R. Cibulka, I. Stibor, M. Yilmaz, *Helv. Chim. Acta* 94 (2011) 481–486.
- [19] E.M. Seward, R.B. Hopkins, W. Sauerer, S.W. Tam, F. Diederich, *J. Am. Chem. Soc.* 112 (1990) 1783–1790.
- [20] M. Mollahosseini, E. Karunaratne, G.N. Gibson, J.A. Gascón, F. Papadimitrakopoulos, *J. Am. Chem. Soc.* 138 (2016) 5904–5915.
- [21] H.A. Staab, M.F. Zipplies, T. Müller, M. Storch, C. Krieger, *Chem. Ber.* 127 (1994) 1667–1680.
- [22] Y. Kamano, Y. Tabata, H. Uji, S. Kimura, *RSC Adv.* 9 (2019) 3618–3624.
- [23] S. Shinkai, H. Nakao, T. Tsuno, O. Manabe, A. Ohno, *J. Chem. Soc., Chem. Commun.* (1984) 849–850.
- [24] S. Shinkai, T. Yamaguchi, O. Manabe, F. Toda, *J. Chem. Soc., Chem. Commun.* (1988) 1399–1401.
- [25] H. Nakade, B.J. Jordan, H. Xu, G. Han, S. Srivastava, R.R. Arvizo, G. Cooke, V.M. Rotello, *J. Am. Chem. Soc.* 128 (2006) 14924–14929.
- [26] J. Žurek, E. Svobodová, J. Šturala, H. Dvořáková, J. Svoboda, R. Cibulka, *Tetrahedron Asymmetry* 28 (2017) 1780–1791.
- [27] S. Shinkai, H. Nakao, I. Kuwahara, M. Miyamoto, T. Yamaguchi, O. Manabe, *J. Chem. Soc. Perkin 1* (1988) 313.
- [28] S. Shinkai, T. Yamaguchi, A. Kawase, A. Kitamura, O. Manabe, *J. Chem. Soc. Chem. Commun.* (1987) 1506.
- [29] A. Khalaj, A. Doroudi, N. Adibpour, G.M. Araghi, *Asian J. Chem.* 21 (2009) 997–1001.
- [30] A. Khalaj, K. Abdi, S. Nasser, M.R. Khoshayand, H.A. Nedaie, *Chem. Biol. Drug Des.* 83 (2014) 183–190.
- [31] M. Miyashita, I. Shiina, T. Mukaiyama, *Bull. Chem. Soc. Jpn.* 67 (1994) 210–215.
- [32] E.C. Butler, A.P. Davis, *J. Photochem. Photobiol. Chem.* 70 (1993) 273–283.
- [33] G. Piersanti, L. Giorgi, F. Bartocchini, G. Tarzia, P. Minetti, G. Gallo, F. Giorgi, M. Castorina, O. Ghirardi, P. Carminati, *Org. Biomol. Chem.* 5 (2007) 2567.
- [34] M. Orlandi, D. Brenna, R. Harms, S. Jost, M. Benaglia, *Org. Process Res. Dev.* 22 (2018) 430–445.
- [35] X. Zhou, X. Wu, B. Yang, J. Xiao, *J. Mol. Catal. Chem.* 357 (2012) 133–140.
- [36] M. Bejugam, S. Sewitz, P.S. Shirude, R. Rodriguez, R. Shahid, S. Balasubramanian, *J. Am. Chem. Soc.* 129 (2007) 12926–12927.
- [37] P. Hemmerich, S. Fallab, H. Erlenmeyer, *Helv. Chim. Acta* 39 (1956) 1242–1252.
- [38] When attempted to reduce an N10 Valine-substituted derivative with Pd/C and FA-Et<sub>3</sub>N, it was observed that the newly formed amine undergoes an intramolecular β-elimination to form a quinoxaline and dihydroquinoxaline. This fast and favourable intramolecular cyclisation is supported by mass spectrometry data from the reaction mixture.
- [39] K. Mallesh, T. Kavitha, V. Malla Reddy, *Acta Cienc. Indica - Phys.* 15 (1989) 67–74.
- [40] P. Kirsch, A. Schönleben-Janasz, R.H. Schirmer, *Liebigs Ann.* 1995 (1995) 1275–1281.

- [41] A.H. Tolba, F. Vávra, J. Chudoba, R. Cibulka, *Eur. J. Org. Chem.* 2020 (2020) 1579–1585.
- [42] J. Shirdel, A. Penzkofer, R. Procházka, J. Daub, E. Hochmuth, R. Deutzmann, *Chem. Phys.* 326 (2006) 489–499.
- [43] E. Sikorska, I.V. Khmelinskii, D.R. Worrall, J. Koput, M. Sikorski, *J. Fluoresc.* 14 (2004) 57–64.
- [44] B. Attenberger, H. Schmaderer, B. König, *Synthesis* 2008 (2008) 1767–1774.
- [45] I. Daidone, A. Amadei, M. Aschi, L. Zanetti-Polzi, *Spectrochim. Acta. A. Mol. Biomol. Spectrosc.* 192 (2018) 451–457.
- [46] M. Spexard, D. Immeln, C. Thöing, T. Kottke, *Vib. Spectrosc.* 57 (2011) 282–287.
- [47] P.F. Heelis, *Chem. Soc. Rev.* 11 (1982) 15–39.
- [48] M.M. Martin, *Chem. Phys. Lett.* 35 (1975) 105–111.
- [49] E. Sikorska, I.V. Khmelinskii, W. Prukala, S.L. Williams, M. Patel, D.R. Worrall, J.L. Bourdelande, J. Koput, M. Sikorski, *J. Phys. Chem.* 108 (2004) 1501–1508.
- [50] H. Masuhara, H. Shioyama, T. Saito, K. Hamada, S. Yasoshima, N. Mataga, *J. Phys. Chem.* 88 (1984) 5868–5873.
- [51] T. Bruhn, A. Schaumlöffel, Y. Hemberger, G. Bringmann, *Chirality* 25 (2013) 243–249.
- [52] J.J.P. Stewart, *J. Mol. Model.* 19 (2013) 1–32.
- [53] F. Neese, *WIREs Comput. Mol. Sci.* 8 (2018), e1327, <https://doi.org/10.1002/wcms.1327>.
- [54] A.-R. Allouche, *J. Comput. Chem.* 32 (2011) 174–182.
- [55] F. Kipnis, N. Weiner, P.E. Spoerri, *J. Am. Chem. Soc.* 69 (1947) 799–800.